OpenNano 1 (2016) 1–15

Contents lists available at ScienceDirect

OpenNano

journal homepage: www.elsevier.com/locate/onano

Full length article

# Optimization and *in-vivo* evaluation of isradipine nanoparticles using Box-Behnken design surface response methodology

Vijayan Venugopal [a,*], K. Jayaraja Kumar [a], S. Muralidharan [c], S. Parasuraman [b], P. Vasanth Raj [a], K. Venkates Kumar [a]

[a] Unit of Pharmaceutical Technology, Faculty of Pharmacy, AIMST University, Malaysia
[b] Unit of Pharmacology, Faculty of Pharmacy, AIMST University, Malaysia
[c] Unit of Pharmaceutical Chemistry, Faculty of Pharmacy, AIMST University, Malaysia

ARTICLE INFO

*Article history:*
Received 7 October 2015
Received in revised form
21 January 2016
Accepted 17 March 2016
Available online 3 May 2016

*Keywords:*
Isradipine
Nanoparticle
Surface response
Box-Behnken design
*In-vivo* studies

ABSTRACT

The isradipine is the potent anti hypertensive drug, which is matrix in polymeric nanoparticle by using solvent evaporation method. In this work, 3-factor, 3-level Box-Behnken design was used to optimize the process parameters like polymer concentration (A), sonication frequency (B) and sonication time (C). Three dependent variable's particle size, entrapment efficiency and practical yield were measured as responses. Mathematical equations and response surface plots were used to relate the dependent and independent variables. The optimization model of particle size of 343.14 nm, entrapment efficiency of about 83.74% and practical yield of 85.39% with A, B and C levels of 750 mg, 37.5 min and 40 kHz respectively. The observed responses were in close agreement with the predicted values of the optimized process. The prepared nanoparticle was characterized by Fourier transform infrared spectroscopy, morphological studies and *in-vitro* drug release studies. The prepared nanoparticle was showed good sustained release of drug upto 24 h. The anti-hypertensive study was performed on animal model. The PMMA (Poly-Methyl-Metha- Acrylate) isradipine nano particle shows fall in blood pressure was delayed and reach 152 ± 2 mmHg at 1 h. The action was sustained until prolong period. Based on pharmacokinetic and pharmacodynamics parameter, the isradipine nanoparticles shows better bioavailability compare with solution form.


## 1. Introduction

Nanoparticles are very small particle's diameter a range is between 100 and 1000 nm [1]. Nanotechnological research is currently applied in various field likes biomedical, electronic and optical [2]. The nano research was initiated in 9th century at mesopotaomia. The artisans used to generate a glittering effect on the surface of pots [3]. Now it is explored by the entire field in worldwide. The use of nanoparticle in biology and medicine including fluorescent biological markers for diagnose of diseases [4] and drug delivery system for all the complicated diseases including genetic diseases. The nanoparticles are being ample use in drug delivery system due to their properties like size, surface characteristics of nanoparticles and its easy adaptability for both active and passive targeting. These particles can be used to control and sustain the release of the drug during the transportation as well as targeted release. These can increase the drug therapeutic efficacy by altering distribution and clearance with significant reduction in side effects [5].

* Correspondence to: Unit of pharmaceutical Technology, Faculty of Pharmacy, AIMST University, Bedong, Kedah, 08100 Malaysia.
*E-mail address:* drvijayan@aimst.edu.my (V. Venugopal).

http://dx.doi.org/10.1016/j.onano.2016.03.002

Isradipine belongs to the dihydropyridine (DHP) class of calcium channel blockers (CCBs), which selectively relaxes coronary, cerebral and skeletal muscle vasculature. Isradipine is a water insoluble calcium channel blocker approved for the treatment of angina pectoris and hypertension. It undergoes significant first-pass metabolism and possess low oral bio-availability (15–24%). The elimination of isradipine is biphasic with an early half-life of 1½ − 2 h, and a terminal half-life of about 8 h. The total body clearance of isradipine is 1.4 L/min and the apparent volume of distribution is 3 L/kg [6].

In this present study, isradipine nanoparticle formula optimized by factorial design software. The optimized formula is subjected to scale up process. Isradipine is low bioavailable, high protein binding and fast elimination molecule. The bioavailability and therapeutic efficacy could be improved by sustained release formulations. In these research isradipine nanoparticles preparation was applied box behnken design model to obtain the optimal formula.

## 2. Materials and methods

The isradipine was obtained from Sigma Aldrich, USA. PMMA (Poly-Methyl-Metha- Acrylate) was obtained from KLH chemicals, Malaysia. Poloxamer 407 and ethanol were purchased from Suka chemicals, SDN BHD, Malaysia. All other chemicals and solvents used were of analytical grade.

### 2.1. Factorial design for formulation of isradipine nanoparticle

Initially, preliminary experiments were performed to determine the main factors and the appropriate ranges in which the optimum range lie. The effects of the three factors (polymer concentration, sonication frequency and sonication time) on the particle size, entrapment efficiency and practical yield were tested. Through preliminary screening the polymer concentration, sonication frequency and sonication time were identified as the most significant variables within the range of 300–1200 mg, 20–60 kHz, 15–60 min, respectively. On the basis of the preliminary trials a 3-factor, 3-level Box-Behnken design [7–9] was employed to study the effect of each independent variable on dependent variables (particle size, entrapment efficiency and practical yield). This design is suitable for exploring quadratic response surfaces and constructing second-order polynomial models. The design consists of replicated centre points and the set of points lying at the midpoint of each edge of the multidimensional cube that defines the region of interest. The independent factors and the dependent variables used in the design are listed in Table 1. The experiments were conducted as for the design of experiments and the responses for the dependent variables were in Table 2. The response surface of the variables inside the experimental domain was analyzed using Stat-Ease design expert software. Subsequently, three additional confirmation experiments were conducted to verify the validity of the statistical experimental strategy.

### 2.2. Preparation of nanoparticle

The isradipine nanoparticle was prepared by solvent evaporation method [10]. The required quantity of isradipine was dissolved in ethanol and the required quantities of polymer PMMA (Poly-Metha-Methyl-Acrylates) was dissolved in dichloromethane. The drug–polymer mixture was added drop wise into 2% poloxamer 407 solution (2 g of poloxamer dissolved in 100 mL of distilled water) as a quasiemulsifier under ultra probe sonication at 20–60 kHz frequency for various time intervals. To complete the precipitation process, 200 mL of water was added and mixed with magnetic stirrer for 12 h. Organic solvent was completely removed by using Rotoevaporator at 40 °C for 30 min. The formed nanoparticles suspension was freeze dried under −20 °C for 26 h to get free flowing powder of nanoparticles.

**Table 1**
List of dependent and independent variables in Box-Behnken design for isradipine nanoparticle.

| Factor | Name | Units | Minimum | Maximum |
|---|---|---|---|---|
| **A** | Polymer | mg | 300 | 1200 |
| **B** | Sonication time | min | 15 | 60 |
| **C** | Sonication frequency | kHz | 20 | 60 |
| Response | Name | Units | | |
| **R1** | Particle size | nm | | |
| **R2** | Entrapment efficiency | % | | |
| **R3** | Practical yield | % | | |

**Table 2**
Central composite design with observed responses.

| Run | Factor 1 A: Polymer | Factor 2 B: Sonication time | Factor 3 C: Sonication Frequency | Response Y1 Particle size | Response Y2 Entrapment efficiency | Response Y3 Practical yield |
|---|---|---|---|---|---|---|
| | mg | min | kHz | nm | % | % |
| **1** | 750 | 37.5 | 40 | 352.12 | 86.42 | 86.3 |
| **2** | 750 | 15 | 20 | 354.24 | 84.22 | 86.4 |
| **3** | 750 | 60 | 20 | 350.4 | 86.06 | 86.6 |
| **4** | 300 | 15 | 40 | 356.62 | 86.42 | 88.64 |
| **5** | 300 | 37.5 | 60 | 356.46 | 78.62 | 88.12 |
| **6** | 300 | 60 | 40 | 358.26 | 89.48 | 88.64 |
| **7** | 1200 | 37.5 | 20 | 367.34 | 86.34 | 78.6 |
| **8** | 300 | 37.5 | 20 | 352.42 | 72.64 | 88.24 |
| **9** | 750 | 15 | 60 | 351.24 | 80.64 | 86.24 |
| **10** | 1200 | 60 | 40 | 360.12 | 82.64 | 72.4 |
| **11** | 750 | 37.5 | 40 | 352.46 | 86.04 | 86.82 |
| **12** | 750 | 37.5 | 40 | 354.22 | 86.4 | 86.42 |
| **13** | 750 | 37.5 | 40 | 356.42 | 82.54 | 81.25 |
| **14** | 1200 | 15 | 40 | 261.42 | 84.64 | 85.02 |
| **15** | 1200 | 37.5 | 60 | 251.4 | 85.06 | 88.32 |
| **16** | 750 | 37.5 | 40 | 356.12 | 86.32 | 87.02 |
| **17** | 750 | 37.5 | 40 | 342.14 | 83.62 | 86.74 |

### *2.3. Characterization of nanoparticles*

#### *2.3.1. Particle size*

Nanoparticles size was determined by using a Zetasizer 300 HS (Malvern Instruments, UK). About 2 mg of samples were dispersed in 2 mL of distilled water and measured the particle size at a temperature of 25 °C. The diameter was calculated from the autocorrelation function of intensity of light scattered from nanoparticles. The values were measured in triplicate.

#### *2.3.2. Entrapment efficiency (EE %)*

Entrapment efficiency was calculated by measuring the quantity of the entrapped drug. The drug samples were analyzed by RP-HPLC (Reverse Phase High Performance Liquid Chromatography) method at 325 nm, which was obtained after ultracentrifugation of nanoparticles suspension [11]. The EE was calculated by using the following formula:

$$\mathrm{EE}(\%) = \frac{W2 - W1}{W1} \times 100$$

where W1 is weight of entrapped drugs, W2 is the total weight of drugs used.

#### *2.3.3. Morphology of nanoparticles*

Morphology of isradipine nanoparticles was observed by scanning electron microscope. A little quantity of nanoparticles sample was spread on a metal stub. The stub was coated with conductive gold by Hitachi 1010 ion sputter and observed under Hitachi 3000N scanning electron microscope (JSM 5610 LV SEM, JEOL, Japan) chamber. The image was snapped at an acceleration voltage of 20 kV with a chamber pressure of 0.6 mmHg.

#### *2.3.4. Compatibility studies*

The isradipine and PMMA compatibility was analyzed by FTIR spectroscopy. The dry nanoparticle power was mixed with 100 mg of potassium bromide (KBr). The sample was compressed to disc by applying pressure of 5 t for 3 min in a hydraulic press. The prepared pellet was placed in the sample cell and the spectrums were analyzed in the region of 4000–400 $cm^{-1}$. By comparing the spectrums of drug and drug loaded nanoparticle, the compatibility study was performed.

#### *2.3.5. In-vitro release study*

*In-vitro* release study of nanoparticle was carried out by using modified Franz diffusion apparatus at $37 \pm 2$ °C. About 50 mg drug equivalent nanoparticles were suspended in donor compartment containing phosphate buffer (pH 7.4). Drug release was assessed by intermittently sampling 5 mL of phosphate buffer as receptor medium and fresh buffer saline pH 7.4 was replaced. The samples were filtered with membrane filter (0.22 μ) and the amount of drug released was quantified by a RP-HPLC method at 325 nm [12].

#### *2.3.6. In-vivo evaluation studies*

*2.3.6.1. Preparation of animals.* Adult male spontaneously hypertensive rats (SHR) were allowed one week to adapt the environmental conditions before all experiments. They were 11–12 weeks old and weighed $220 \pm 20$ g when experiments were performed.

*2.3.6.2. Experiment.* Isradipine was administered to rat at a dose of 12 mg/kg in one of the 2 forms (Pure isradipine, PMMA nanoparticle loaded isradipine and plain nanoparticle). The dosing volume was 5 mL/kg and there were 6 SH (Spontaneously Hypertensive) rats per group. Measurements of rat systolic arterial blood pressure were fasted for 15 h before and during the experiments; water was given ad libitum. Systolic arterial blood pressure was measured by tail plethysmography at 0, 15 min, 0.5, 1, 2, 4, 8 and 12 h following oral administration of nanoparticles.

*2.3.6.3. Blood sampling.* The common carotid artery of separate groups of rat was cannulated under halothane anaesthesia [13]. The cannula was labelled with a solution containing poly vinylpyrrolidone (PVP) (0.5 mg/mL), heparine (200 i. u/mL), sodium chloride (90 mg/mL) and methylene blue. A minute quantity of methylene blue (51 mg/L) was added in order to give a blue colour to the solution used to label the cannula. In this way any leak from the cannula could easily be detected. The cannula was sealed and rats were housed in individual cages. Experiments were performed 15 h later. Blood samples were withdrawn at 0, 15 min, 0.5, 1, 2, 4, 8, 10 and 12 h after oral administration of each dosage form (Pure isradipine, PMMA nanoparticle loaded isradipine & plain nanoparticle). Blood samples were centrifuged at 1500*g* for 10 min at 48 °C and the plasma samples were analyzed immediately by RP-HPLC.

*2.3.6.4. Analytical methods.* Reversed phase HPLC method was chosen for isradipine. HPLC chromatographic separation was performed on a shimadzu liquid chromatographic system equipped with a LC-20CE solvent delivery system (pump), SPD-20A photo diode array detector, and SIL-20ACHT injector. LC solution version 1.25 was applied for data collecting and processing (Shimadzu, Japan). Isradipine plasma samples (100 mL), 4 mL of a dichloromethane: n hexane mixture (3: 7, v/v) and 1 mL of distilled water were mixed in a light-proof test tube. The mixture was shaken for 15 min with a rotary agitator and centrifuged for 5 min at 1500*g*. Three millilitres of the supernatant were transferred to a light-proof reaction. The residue was dissolved in 200 mL of the mobile phase containing n-butyl p-aminobenzoate (butamben) as internal standard (500 mg/mL). 05 mM ammonium acetate buffer (pH 4.5) and acetonitrile at a ratio of 30:70% v/v was used as the mobile phase with the flow rate of 1.0 mL/min. Reversed phase thermos $C_{18}$ column was used as the stationary phase. The flowrate was 1.0 mL/min and the detection wavelength of isradipine was 325 nm.

*2.3.6.5. Statistical analysis.* Analysis of variance (ANOVA) and linear regression analysis were performed on the blood pressure and plasma isradipine data. Means were compared with the Bonferroni test. Differences were considered significant at $P < 0.05$.

## 3. Results and discussion

### *3.1. Optimization process variables of isradipine nanoparticles*

The most widely used method for the synthesis of the nanoparticle is the solvent evaporation method; potential advantages of this technique in the synthesis of biodegradable materials include the acceleration of nanoparticle formation, improved product selectivity, narrow particle size distribution and high yield. In this work, we report the first successful result on the preparation of isradipine nanoparticle. Through preliminary experiments the polymer concentration (A), sonication frequency (B) and sonication time(C) were identified as the most significant variables influence the particle size, entrapment efficiency and practical yield.

Design of experiments (DOE) has been used as a powerful approach to reduce the variation in a process and, ultimately, to produce high product yield with uniform particle size distribution. Among various design approaches, the Box-Behnken design was used to optimize and evaluate main effects, interaction effects and quadratic effects of the process variables on the particle size, entrapment efficiency and practical yield. This design is suitable for exploring quadratic response surfaces

**Table 3**
ANOVA results of the quadratic model for the response particle size (Y1).

| Sources of variations | Sum of squares | df | Mean square | F value | p-Value Prob > F | $R^2$ |
|---|---|---|---|---|---|---|
| **Model** | 13019.88 | 6 | 2169.98 | 4.82 | 0.0145 | Significant |
| ***A - Polymer*** | *4208.11* | *1* | *4208.11* | *9.35* | *0.0121* | |
| ***B - Sonication time*** | *954.85* | *1* | *954.85* | *2.12* | *0.1759* | |
| ***C - Sonication Frequency*** | *1896.05* | *1* | *1896.05* | *4.21* | *0.0672* | |
| ***AB*** | *2355.16* | *1* | *2355.16* | *5.23* | *0.0452* | |
| ***AC*** | *3598.80* | *1* | *3598.80* | *8.00* | *0.0179* | |
| ***BC*** | *6.92* | *1* | *6.92* | *0.015* | *0.9038* | |
| **Residual** | 4499.96 | 10 | 450.00 | | | |
| ***Lack of Fit*** | *4484.02* | *6* | *747.34* | *187.47* | *< 0.0001* | *Significant* |

**Table 4**
ANOVA results of the quadratic model for the response Entrapment efficiency (Y2).

| Sources of variations | Sum of squares | df | Mean square | F value | p-Value Prob > F | $R^2$ |
|---|---|---|---|---|---|---|
| **Model** | 0.000 | 0 | | | | |
| **Residual** | 241.76 | 16 | 15.11 | | | |
| ***Lack of Fit*** | *230.38* | *12* | *19.20* | *6.75* | *0.0397* | *Significant* |

**Table 5**
ANOVA results of the quadratic model for the response Practical yield (Y3).

| Sources of variations | Sum of squares | df | Mean square | F value | p-Value Prob > F | $R^2$ |
|---|---|---|---|---|---|---|
| **Model** | 136.54 | 3 | 45.51 | 3.88 | 0.0350 | Significant |
| ***A - Polymer*** | *107.31* | *1* | *107.31* | *9.15* | *0.0098* | |
| ***B - Sonication time*** | *17.76* | *1* | *17.76* | *1.51* | *0.2403* | |
| ***C - Sonication Frequency*** | ***11.47*** | *1* | *11.47* | *0.98* | *0.3407* | |
| **Residual** | 152.48 | 13 | 11.73 | | | |
| ***Lack of Fit*** | *128.90* | *9* | *14.32* | *2.43* | *0.2037* | *Significant* |

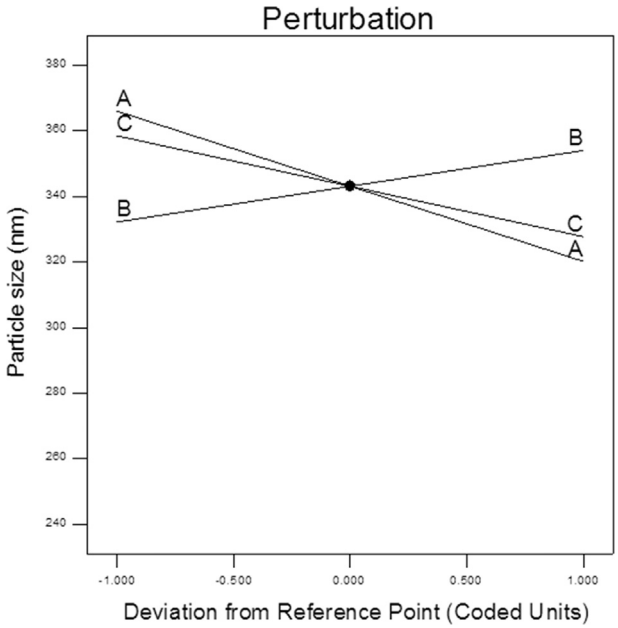


**Fig. 1.** Perturbation plot showing the main effect of Polymer concentration (A), Sonication frequency (B) and sonication time (C) on Particle size (Y1).

and constructing second order polynomial models. The design consists of replicated centre points and the set of points lying at the midpoint of each edge of the multidimensional cube. These designs are rotatable (or near rotatable) and require 3 levels of each factor.

Seventeen experiments were required for the response surface methodology based on the Box-Behnken design. Based on the experimental design, the factor combinations yielded different responses as presented in Table 1. These results clearly indicate that all the dependent variables are strongly dependent on the selected independent variables as they show a wide variation among the 17 batches (Table 2). Data were analyzed using Stat-Ease Design Expert software to obtain analysis of variance (ANOVA), regression coefficients and regression equation. Mathematical relationship generated using multiple linear regression analysis for the studied variables are expressed. These equations represent the quantitative effect of polymer concentration (A), sonication frequency (B) and sonication time(C) and their interaction on particle size (Y1), entrapment efficiency (Y2) and practical yield (Y3). The values of the coefficient A, B and C are related to the effect of these variables on the responses Y1, Y2 and Y3. Coefficients with more than one factor term and those with higher order terms

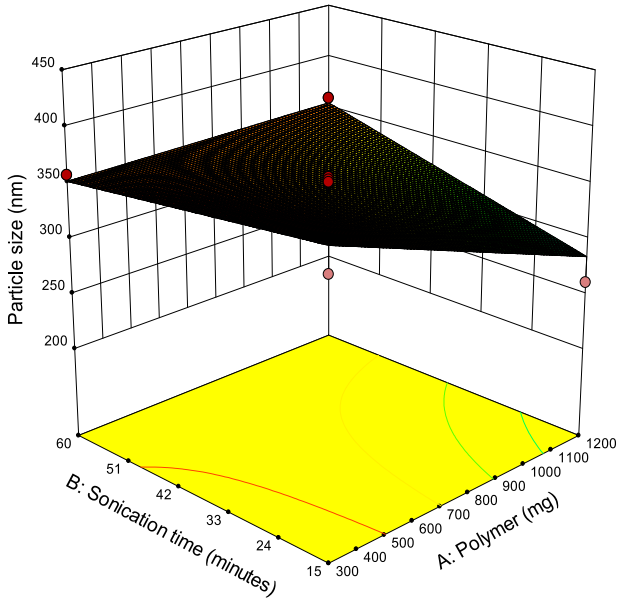


**Fig. 2.** Response surface plot presenting the interaction between the Polymer and Sonication time affecting the particle size at constant sonication frequency.

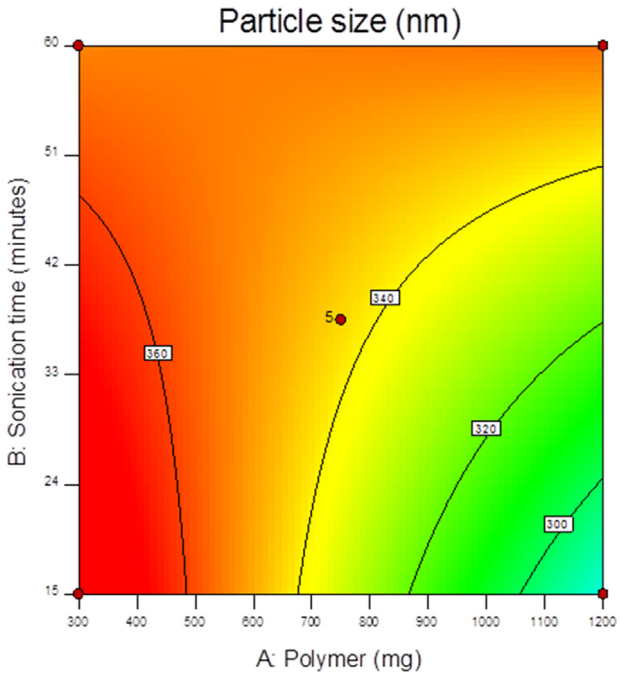


**Fig. 3.** Factorial contour Response surface plot presenting the interaction between the Polymer and Sonication time affecting the particle size at constant sonication frequency.

represent interaction terms and quadratic relationship respectively. A positive sign represents a synergistic effect, while a negative sign indicates an antagonistic effect. A backward elimination procedure was adopted to fit the data to the quadratic model. All the polynomial equations were found to be statistically significant ($P < 0.014$), as determined using ANOVA (Tables 3–5), as per the provision of design expert software. The mathematical model generated for practical yield (Y1) was found to be significant with F-value of 4.82 ($p < 0.0005$) and $R^2$ value of 0.9942. The independent variables A, B, C and the quadratic term of AB, AC and BC have significant effects on the particle size, since the P-values less than 0.05 represent the significant model terms as shown in Table 3. Results of the equation indicate that the effect of A is more significant than B and C.

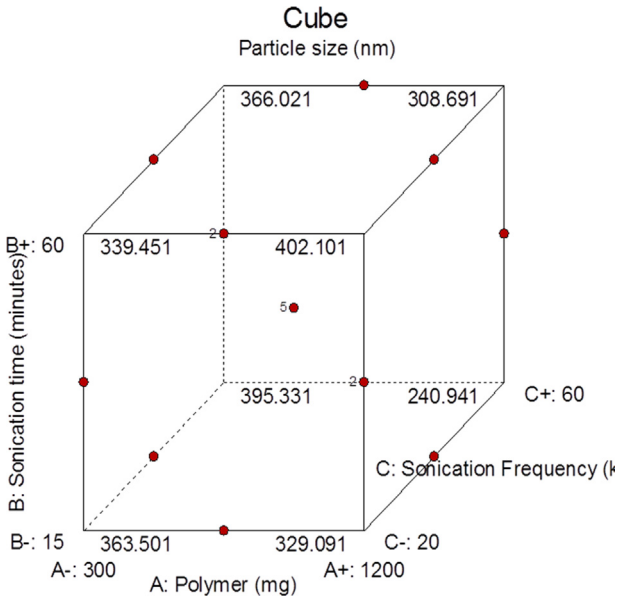


**Fig. 4.** Cubic design presenting the interaction between the Polymer and Sonication time and sonication frequency affecting the Particle size.

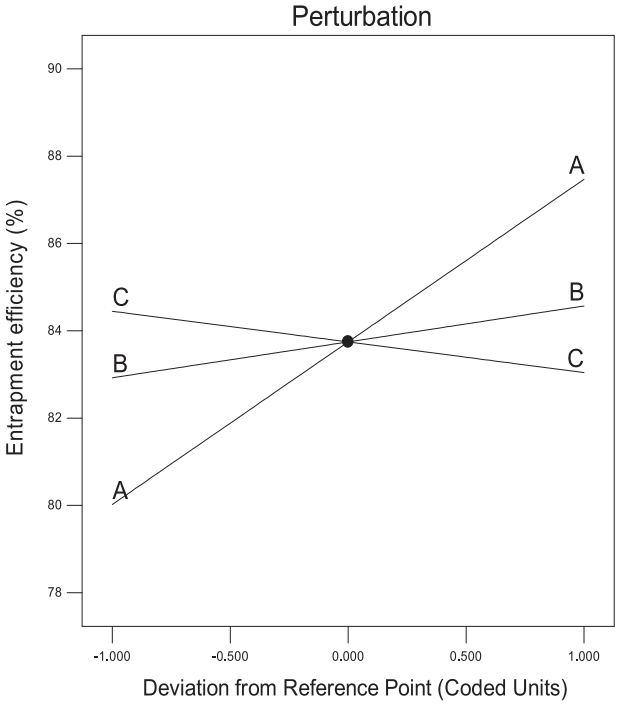


**Fig. 5.** Perturbation plot showing the main effect of Polymer concentration (A), Sonication frequency (B) and sonication time (C) on entrapment efficiency (Y2).

The influence of the main and interactive effects of independent variables on the particle size was further elucidated using the perturbation and 3D response surface plots. The perturbation plot (Fig. 1) showing the main effects of A, B and C on the particle size (Y1) of nanoparticle. This figure clearly shows that A has the main and the major effect on Y1 followed by B which has a moderate effect on Y1 followed by C which has a little effect on Y1. The relationship between the dependent and independent variables was further elucidated using response surface plots in Fig. 2. Figs. 3 and 4 shows the interactive effect of A and B on the particle size (Y1) at fixed level of C. At low levels of A (polymer concentration), Y1 increases from

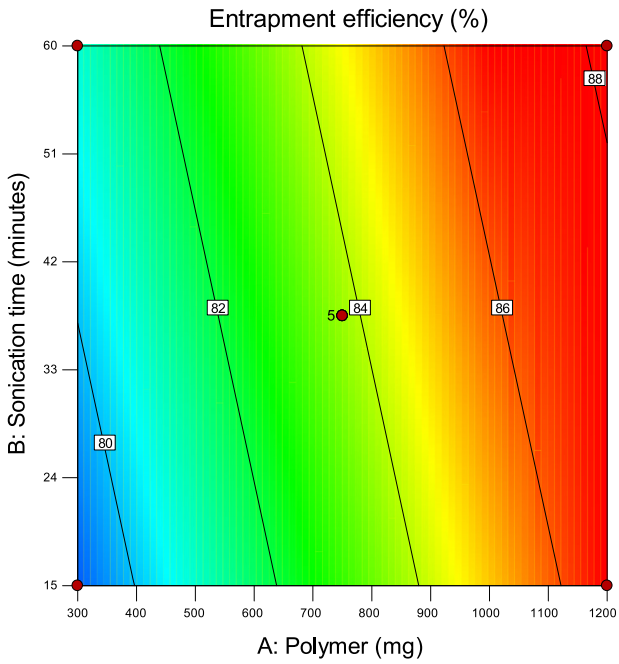


**Fig. 6.** Factorial contour Response surface plot presenting the interaction between the Polymer and Sonication time affecting the Entrapment efficiency at constant sonication frequency.

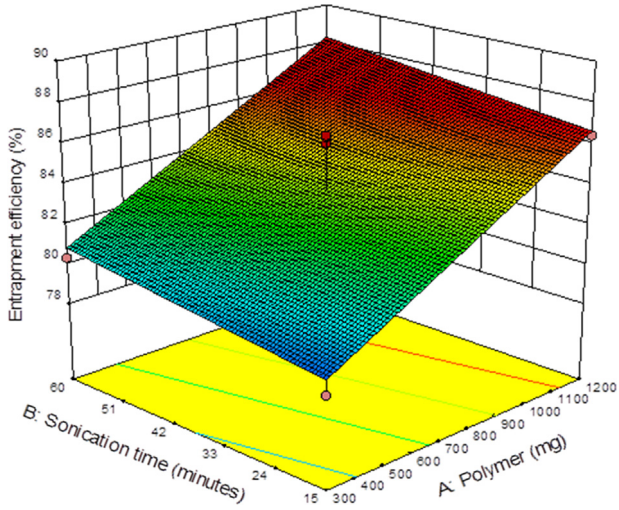


**Fig. 7.** Response surface plot presenting the interaction between the Polymer and Sonication time affecting the Entrapment efficiency at constant sonication frequency.

352 nm to 358 nm. Similarly, at high levels of A, Y1 increases from 251 nm to 367 nm. Particle size analysis of nanoparticle was found to be in the range of 251–367 nm as shown in Table 2. The factorial equation for particle size exhibited a good correlation coefficient (1.000) and the model F value of 187.47 which implies the model is significant. Values of "Prob $>$ F" less than 0.0500 indicate model terms are significant. All the three variables having the negative effect on the particle size, which means these factors, are inversely proportional to the response. The influence of the main and interactive effects of independent variables on the particle size was further elucidated using the perturbation and 3D response surface plots.

The individual main effects of A, B and C on entrapment efficiency are as shown in Fig. 5. It is found that all the variables are having interactive effects for the response Y2. The 3D response surfaces and the 2D contour plots of the response Y2 are shown in Figs. 6–8 and to depict the interactive effects of independent variables on response Y2, one variable was kept constant while the other two variables varied in a certain range. The shapes of response surfaces and

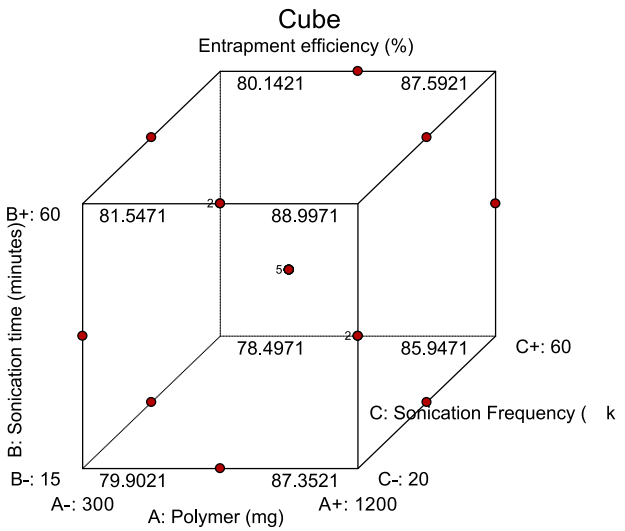


**Fig. 8.** Cubic design presenting the interaction between the Polymer and Sonication time and sonication frequency affecting the Entrapment efficiency.

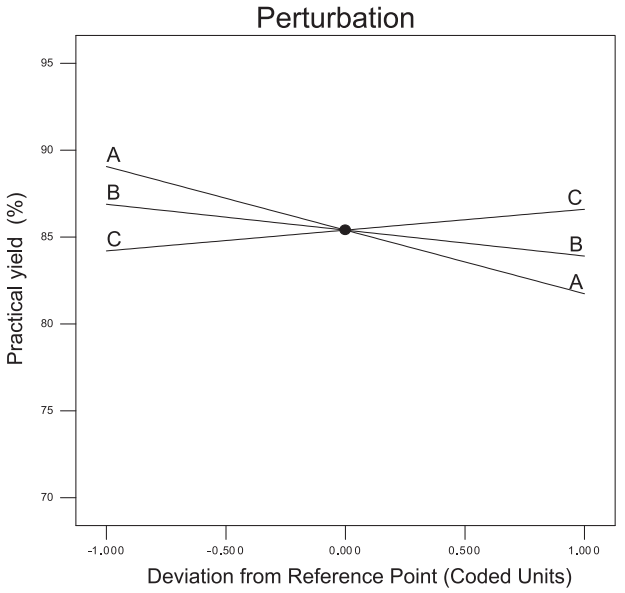


**Fig. 9.** Perturbation plot showing the main effect of Polymer concentration (A), Sonication frequency (B) and sonication time (C) on Practical yield (Y3).

contour plots reveal the nature and extent of the interaction between different factors. At low levels of A, Y2 reduced from 89 to 72%. Similarly at high levels of A, Y2 reduced from 86 to 82%. The interaction between A and C on practical yield at a fixed level of C is shown in Fig. 8 and the interaction between A and B on practical yield at a fixed level of B. At low levels of A, Y3 reduced from 88.64 to 88.12%. Similarly at high levels of A, Y3 reduced from 88 to 78%. After generating the polynomial equations relating the dependent and independent variables, the process was optimized for the responses (Fig. 9). Numerical optimization using the desirability approach was employed to locate the optimal settings of the process variables to obtain the desired responses (Figs. 10–12). Optimized conditions were obtained by setting constraints on the dependent and independent variables. Optimization was performed to obtain the levels of A-C which maximize Y1, Y2 and Y3. The optimized levels and predicted values of Y1, Y2 and Y3 are shown in Table 6.

Based on the factorial design studies, the optimized formulation of Isradipine nanoparticle was founded in Table 6. The optimized formula showed better particle size, entrapment efficiency and practical yield i. e. 343 nm and 83% and 85% respectively. To verify these values, three batches of nanoparticle was prepared according to the predicted level of A, B and C. obtained Y1, Y2 and Y3 values were in a closed agreement with the predicted values as shown in Table 2. This demonstrated the reliability of optimized procedure in predicting the operating parameters for the preparation of isradipine nanoparticle. The selected formulation was subjected to *invitro* release studies.

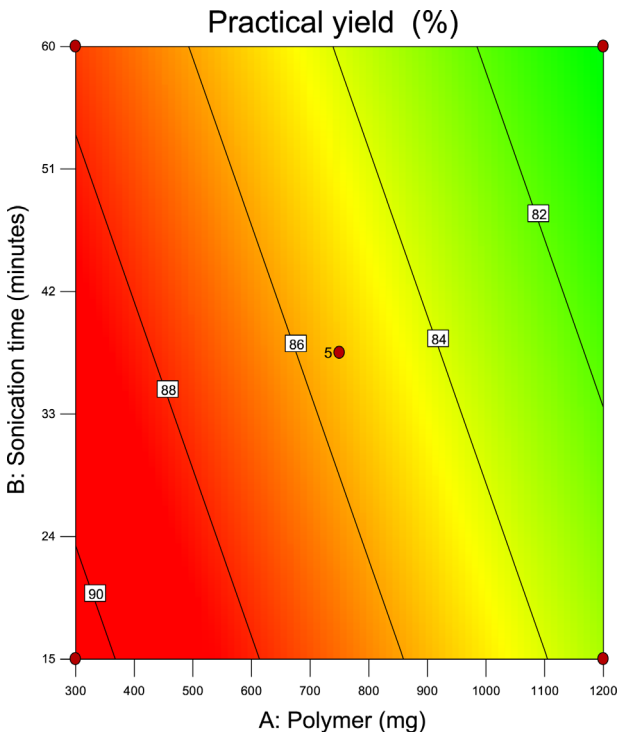


**Fig. 10.** Factorial contour Response surface plot presenting the interaction between the Polymer and Sonication time affecting the Practical yield at constant sonication frequency.

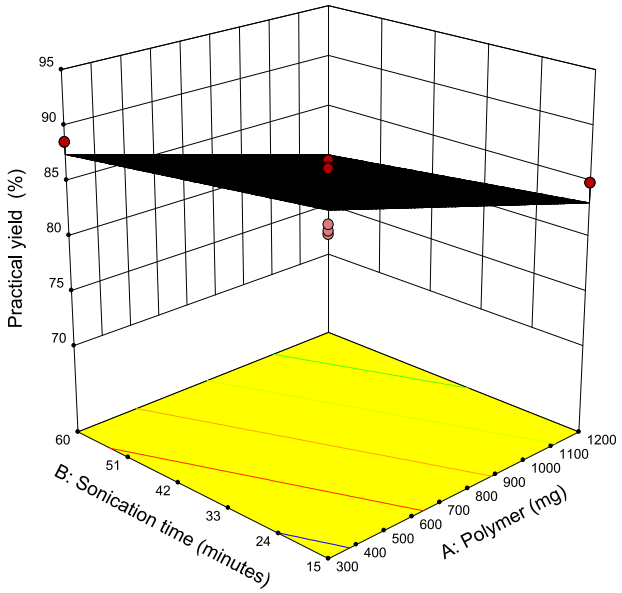


**Fig. 11.** Response surface plot presenting the interaction between the Polymer and Sonication time affecting the Practical yield at constant sonication frequency.

### *3.2. Preparation and characterization of isradipine nanoparticles*

The isradipine nanoparticles were prepared by solvent evaporation method with PMMA as biodegradable polymers. This method was comparatively easy to prepare than other methods. During the preparation of nanoparticle, the aqueous and organic phase was emulsified completely to form spherical shaped particles. The stability was provided by quasi-emulsifier.

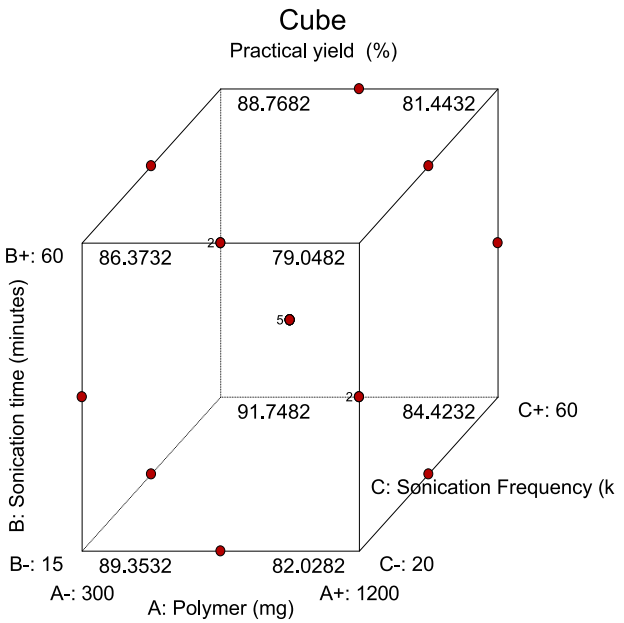


**Fig. 12.** Cubic design presenting the interaction between the Polymer and Sonication time and sonication frequency affecting the Practical yield.

**Table 6**
Optimized isradipine nanoparticle values obtained by the constraints applies on Y1, Y2 and Y3.

| Independent variables | Values | Predicted values | | | Observed values | | |
|---|---|---|---|---|---|---|---|
| | | Globule size (Y1) | EE (Y2) | Practical Yield (Y3) | Globule size (Y1) | EE (Y2) | Practical Yield (Y3) |
| Polymer | 750.00 | 343.14 | 83.74 | 85.39 | 346.2 | 84.32 | 84.94 |
| Sonication time | 37.50 | | | | | | |
| Sonication Frequency | 40.00 | | | | | | |

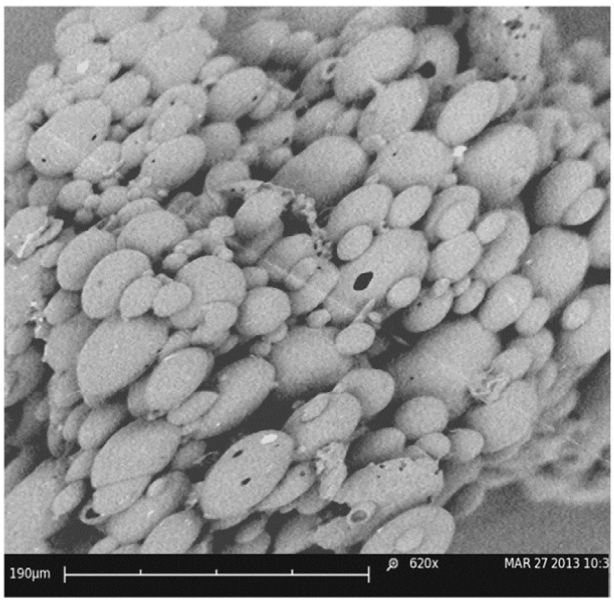


**Fig. 13.** SEM image of Isradipine nanoparticle.

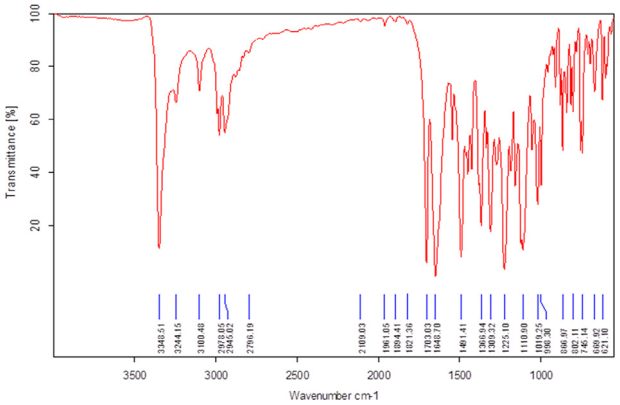


**Fig. 14.** FTIR Spectrum of pure Isradipine.

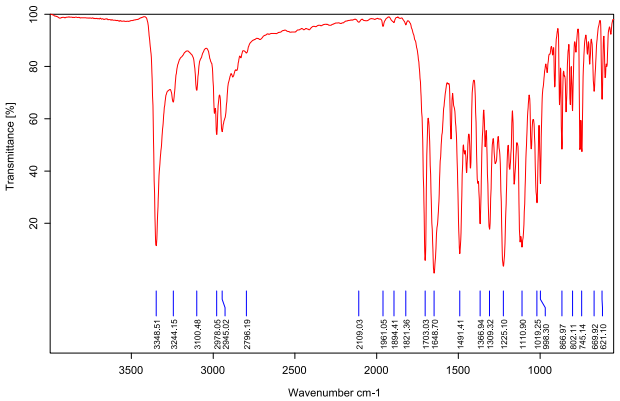


**Fig. 15.** FTIR Spectrum of Isradipine nanoparticle.

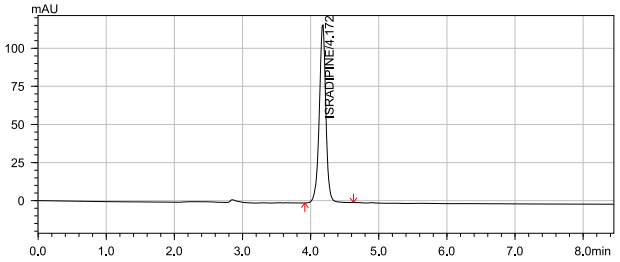


**Fig. 16.** Typical chromatogram of isradipine standard.

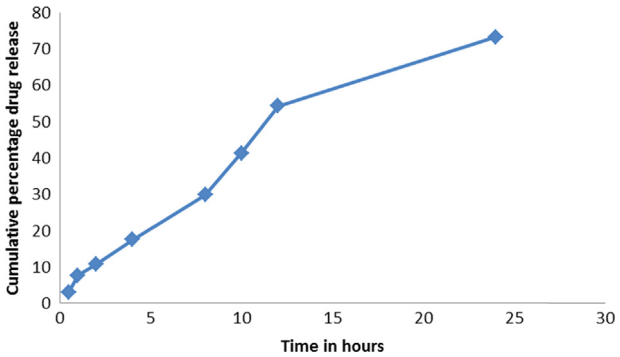


**Fig. 17.** *Invitro* drug release of Isradipine nanoparticle.

**Table 7**
Pharmacokinetics Parameters of isradipine nanoparticle.

| S. no. | Parameters | Isradipine solution (oral) | Isradipine nanoparticle |
|---|---|---|---|
| **1** | Cmax (ng/mL) | 702 | 1502 |
| **2** | Tmax (h) | 0.25 | 0.5 |
| **3** | T1/2 (h) | 4.81 | 150.54 |
| **4** | AUC (ng/mL h) | 3919.87 | 10011.75 |
| **5** | AUMC (ng/mL $h^2$) | 30315.61 | 40230737.71 |
| **6** | MRT (h) | 6.6 | 217.12 |
| **7** | Clearances ((ng/mL)/h) | 0.002 | 6.74 |

AUC – Area under curve, AUMC – Area under moment curve, MRT – Mean residential time.

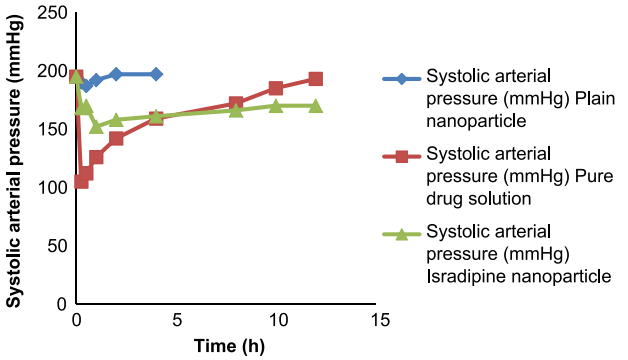


**Fig. 18.** *In-vivo* antihypertensive studies of isradipine nanoparticles.

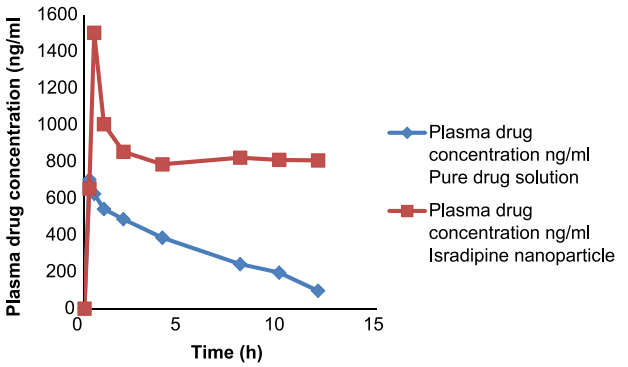


**Fig. 19.** Plasma concentration of isradipine nanoparticles.

After the formation of nanoparticle, the organic solvent was completely removed by rota-evaporation at 40 °C for 30 min. The nanoparticles were dried by freeze dryer at −20 °C for 26 h to get free flowing power of drug loaded nanoparticles. The dried nanoparticle was stored in freeze condition for further studies. The optimized formulation of nanoparticles showed smooth and spherical shape (Fig. 13). These shape was produced by fully saturated of polymer and the diffusion rate of solvent was minimal, leading to formation of smooth, spherical and homogeneously distributed particles, which has smooth surface and the solvent was completely removal from the nanoparticles.

The FTIR studies showed (Figs. 14 and15) that the significant peaks of isradipine are C N stretching at 1226 $cm^{-1}$, C-O vibration at 1648 $cm^{-1}$, N-H at 3439 $cm^{-1}$, O H vibration at 3626 cm-1 and C=C vibration at 3244 $cm^{-1}$. Finally the FTIR studies of mixture of polymers and drug does not show any significant change. This result indicates that there are no any interactions between drug and polymers.

The optimized nanoparticle formulation subjected to *in-vitro* drug release study using pH 7.4 phosphate buffers and the isradipine was analyzed by RP-HPLC at 325 nm (Fig. 16). The drug release was initially bust followed by sustained release. Initially 2.8% drug release at 30 min and sustained release of 73% at 24th h (Fig. 16). The initial bust release was produced by surface adhered drug particles and the sustained release due to release from polymeric matrix (Fig. 17).

### 3.3. In-vivo evaluation studies

Administration of empty PMMA nanoparticle had no significant effect on systolic arterial blood pressure. After oral administration of the isradipine solution, systolic arterial blood pressure fell very rapidly from $195 \pm 3$ mmHg to $105 \pm 2$ mmHg at 0.25 h, and then returned rapidly to a value not significantly different from the pre-injection value ($193 \pm 3$ mmHg) at 12 h. After administration of isradipine nanoparticles, systolic arterial blood pressure fell gradually and the maximal antihypertensive effect ($152 \pm 2$ mmHg) was obtained at 1 h. At 10 h the systolic arterial blood pressure in the PMMA group ($170+3$ mmHg) was no different from that point (Fig. 18).

Blood pressure initially fell to a value less than the lower limit of cerebral blood flow autoregulation for approximately 15 min, extending these data to human, daily repetition of such periods of iatrogenic cerebral ischaemia over several years could have a very detrimental effect on brain functions. With the PMMA nanoparticle preparation the fall in blood pressure was delayed and the nadir reached (at 1 h) $152 \pm 2$ mmHg was well above the value for the lower limit of cerebral blood flow autoregulation. The polymer loaded isradipine nanoparticle were sustained the drug release form the matrix, these leads to optimized control of hypertensive action.

Based on plasma concentration time profile (Fig. 19), pharmacokinetic parameters were calculated by using PK solver software. The pharmacokinetics parameters Cmax, Tmax, AUC, AUMC, MRT, t1/2 and clearances of isradipine solution (oral) were 702 ng/mL, 2 h, 0.25 h, 3919.87 ng/mL h, 30315.61 ng/mL $h^2$, 4.8 h and 0.002 ng/mL/h respectively. In case of isradipine nanoparticle formulation showed 1502 ng/mL, 0.5 h, 10011.75 ng/mL h, 40230737.7 ng/mL $h^2$, 217.1 h and 6.7 ng/mL/h, respectively (Table 7). These pharmacokinetics values indicated that, isradipine concentration was significantly maintained throughout the time period. Isradipine nanocarriers shows increased Cmax, mean residence time (MTR), AUC and AUMC. The increase in Cmax can be explained by the slow diffusion of the drug from the nanoparticles. This may explain the decrease in the initial antihypertensive effect with the nano forms, especially PMMA which showed a plasma level between 2 and 3 times less than that of the isradipine solution. The *invivo* antihypertensive studies of isradipine nanoparticle shows effective therapeutics concentration in blood when compare to isradipine pure form.

## 4. Conclusion

In this research we tried isradipine nanoparticle preparation by solvent evaporation method and optimized by 3-level factorial design studies. From preliminary experiments, the polymer concentration (A), sonication frequency (B) and sonication time (C) were identified as the most significant variables which influence the particle size, entrapment efficiency and practical yield. The quantitative effect of these factors at different levels was predicted by using polynomial equations. Response surface methodology was then used to predict the optimum levels of these factors to obtain nanoparticles with uniform particle size and high entrapment efficiency and practical yield. One formulation of nanoparticle was prepared according to these optimized levels. Observed responses were in close agreement with the predicted values of the optimized process, thereby demonstrating the feasibility of the optimization procedure for preparation of isradipine nanoparticles. The factorial design provides a unique opportunity for the large-scale preparation of isradipine nanoparticle with uniform particle size distribution with high entrapment efficiency and practical yield. The *in vivo* antihypertensive studies of isradipine nanoparticle shows effective therapeutics concentration in blood when compare to isradipine pure form. Based on pharmacokinetic assessment, isradipine nanoparticle shows effective therapeutic concentration compare with pure solution form.

## Acknowledgment

Authors are thankful to AIMST University, Malaysia for providing the facilities and declared that they have no conflict of interest.

## References

[1] C.G. Granqvist, R.A. Buhrman, J. Wyns, A.J. Sievers, Far-Infrared absorption in ultrafine Al particles, Phys. Rev. Lett. 37 (1976) 625–629.
[2] Cristina Buzea, Ivan Pacheco, Kevin Robbie, Nanomaterials and nanoparticles: sources and toxicity, Biointerphases 2 (2007). MR17–MR71.
[3] S. Philip, Rawson, Ceramics, second ed. University Of Pennsylvania Press, Reissue, 1984.
[4] Z. Bruche, M. Moronne, P. Gin, S. Weiss, A.P. Alivisatos, Semiconductor nanocrystals as fluorescent biological labels, Science 281 (1998) 2013–2016.
[5] B.K. Krfimer, M.H. Iussler, K.M. Ress, G.A. Mtfller, K.J. Burger, T. Risler, Renal effects of the new calcium channel blocking drug isradipine, Eur. J. Clin. Pharmacol. 39 (1990) 333–335.
[6] H.R. Christensen, K. Antonsen, K. Simonsen, A. Lindekaer, J. Bonde, H.R. Angelo, J.P. Kampmann, Bioavailability and pharmacokinetics of isradipine after oral and intravenous administration: half-life shorter than expected, Pharmacol. Toxicol. 86 (2000) 178–182.
[7] C. Mah, T. Zolotukhin, T.J. Fraites, J. Dobson, C. Batich, B.J. Byrne, Improved method of recombinant AAV2 delivery for systemic targeted gene therapy, Mol. Ther. 6 (2002) 106–112.
[8] S. Swaminathan, L. Pastero, L. Serpe, F. Trotta, P. Vavia, D. Aquilano, G. Trotta, G. Zara, R. Cavalli, Cyclodextrin-based nanosponges encapsulating camptothecin: physicochemical characterization, stability and cytotoxicity, Eur. J. Pharm. Biopharm. 74 (2010) 193.
[9] S. Swaminathan, P.R. Vavia, F. Trotta, R. Cavalli, S. Tumbiolo, L. Bertinetti, A. Coluccia, Structural evidence of differential forms of nanosponges of beta-cyclodextrin and its effect on solubilization of a model drug, J. Incl. Phenom. Macrocycl. Chem. 76 (2013) 201.

[10] Sung Hwa Jhung, Jin.-Ho. Lee, Jong.-San. Chang, Microwave synthesis of a nanoporous hybrid material, chromium trimesate, Bull. Korean Chem. Soc. 26 (2005) 880–881.
[11] H. Su, H. Xu, S. Gao, J.D. Dixon, Z.P. Aguilar, A.Y. Wang, J. Xu, J. Wang, Microwave-assisted aqueous synthesis of small-sized, highly luminescent CdSeS/ZnS core/shell quantum dots for live cell imaging, Nanoscale Res. Lett. 5 (2010) 625.
[12] T.T. Tran, P.H. Tran, M.N. Nguyen, K.T. Tran, M.N. Pham, P.C. Tran, T.V. Vo, Amorphous isradipine nanosuspension by the sono-precipitation method, Int. J. Pharm. 474 (2014) 146–150.
[13] S. Parasuraman, R. Raveendran, Measurement of Invasive blood pressuresun rats, J. Pharmacol. Pharmacother. 3 (2012) 172–177.